Growth shapes of supported Pd nanocrystals on $SrTiO_3(001)$

Fabien Silly, Andrew C. Powell, Marta G. Martin, and Martin R. Castell
Department of Materials, University of Oxford, Parks Road, Oxford OX1 3PH, United Kingdom
(Received 13 July 2005; published 3 October 2005)

Pd is deposited onto a reconstructed $SrTiO_3(001)$ substrate in an ultrahigh vacuum environment. Elevated substrate temperature during or following deposition causes epitaxial Pd nanocrystals to form. The nanocrystal shape and size distributions are analyzed by scanning tunneling microscopy. We find that depending on substrate reconstruction and substrate temperature during deposition three shapes of nanocrystal are obtained: truncated pyramids, huts, and hexagonal shaped disks. In our previous study [F. Silly and M. R. Castell, Phys. Rev. Lett. **94**, 046103 (2005)] the energetics of the equilibrium nanocrystal shapes were analyzed. Here we report on the nonequilibrium growth shapes. We show that preferential growth for huts is along their (001) end facets. For hexagons growth proceeds by attachment to the side of the crystals. Truncated pyramids can grow preferentially along one of their (111) side facets resulting in an elongated shape.

DOI: 10.1103/PhysRevB.72.165403 PACS number(s): 68.47.Jn, 68.37.Ef, 75.70.Kw

I. INTRODUCTION

Metal nanocrystals on oxide substrates are of interest for use in a wide variety of applications, such as catalysis, electronics, optoelectronics, optics, and magnetic storage.[2–6] For these applications functionality can be improved if the nanocrystals have a precise morphology and crystallographic orientation. Extensive studies have been undertaken into the metal-oxide interface and to monitor the growth of small islands.[7,8] Many factors can affect the structure and morphology of metal nanocrystals grown on metal oxides. The crystallography of the substrate and the interface energy between the metal and the oxide substrate determine the shape of the nanocrystals.[1] Kinetic factors during growth are critical in determining the distribution and size of the clusters.

Interest in the $SrTiO_3$ surface has emerged from its electronic properties[14] and its use as a substrate for growth of oxides, including layered high-T_c superconductors[9–11] and metals.[1,12,13,15] Applications in microelectronics involving $SrTiO_3$ as an alternative gate dielectric or a buffer material between Si and GaAs have further stimulated research into this material. At room temperature $SrTiO_3$ exists in the cubic perovskite structure with a 3.905 Å lattice parameter, but transforms into the tetragonal structure at temperatures below 105 K. At very low temperatures, $SrTiO_3$ exhibits piezoelectric and superconducting characteristics. It also exhibits a very large dielectric constant.

Pd is widely used in supported small particle form for hydrogenation reactions in heterogenous catalysis. In its crystalline state Pd adopts the face centered cubic structure with a lattice parameter of 3.890 Å. The lattice mismatch between $SrTiO_3$ and Pd is therefore only 0.4%. Pd thin films and nanocrystals can be grown epitaxially on $SrTiO_3$ surfaces.[15] Moreover, it was recently shown that it is possible to select the shape of Pd nanocrystals through the choice of $SrTiO_3$ surface reconstruction and sample temperature.[1,16] In this paper, we report a scanning tunneling microscopy (STM) investigation of the shape of Pd nanocrystals grown away from equilibrium on $SrTiO_3(001)$.

II. EXPERIMENTAL PROCEDURES

In its pure form $SrTiO_3$ has a 3.2 eV band gap which would make it unsuitable for imaging in the scanning tunneling microscope (STM). To overcome this problem we use crystals doped with 0.5% (weight) Nb. We deposited Pd from an electron-beam evaporator (Oxford Applied Research EGN4) using 99.95% pure Pd rods supplied by Goodfellow, UK. Our STM is manufactured by JEOL (JSTM 4500s) and operates in UHV (10^{-8} Pa). We used etched W tips to image the samples at room temperature with a bias voltage applied to the sample. $SrTiO_3(001)$-(2×1) reconstructed surfaces were prepared by chemically etching the crystals in a buffered NH_4F-HF solution and subsequently annealing in UHV at 800 °C for 30 min. Surfaces with a $c(4\times2)$ reconstruction were obtained by Ar^+ sputtering, typically at 500 eV for 10 min, followed by a 900 °C anneal for 30 min. A detailed account of surface preparation and characterization is described in the paper by Castell.[17]

III. RESULTS

A. Pd nanocrystals on $SrTiO_3(001)$-(2×1): Huts

Around two monolayers of palladium were deposited in three separate experiments on $SrTiO_3(001)$-(2×1) surfaces at substrate temperatures of room temperature, 320 and 415 °C. The depositions were all followed by a 45 min anneal at 650 °C. Figure 1 shows that Pd forms hut shaped nanocrystals on the (2×1) reconstruction. A model of this shape is presented in Fig. 2(a). These nanocrystals have a rectangular base which is aligned along the <100> crystallographic directions of the $SrTiO_3$ substrate. The nanocrystal facet angles are measured to be inclined at ~46° with respect to the substrate for the end facets and ~37° for the side facets. The hut nanocrystals therefore have an (011) interface with (001) end facets and (111) side facets and the interfacial crystallography is $(011)_{Pd}\|(001)_{SrTiO_3}, [110]_{Pd}\|[100]_{SrTiO_3}$. The sample during Pd deposition was at room temperature for Fig. 1(a), at 320 °C for Fig. 1(b), and at 650 °C for Fig. 1(c). All depositions were followed by a 650 °C postanneal.

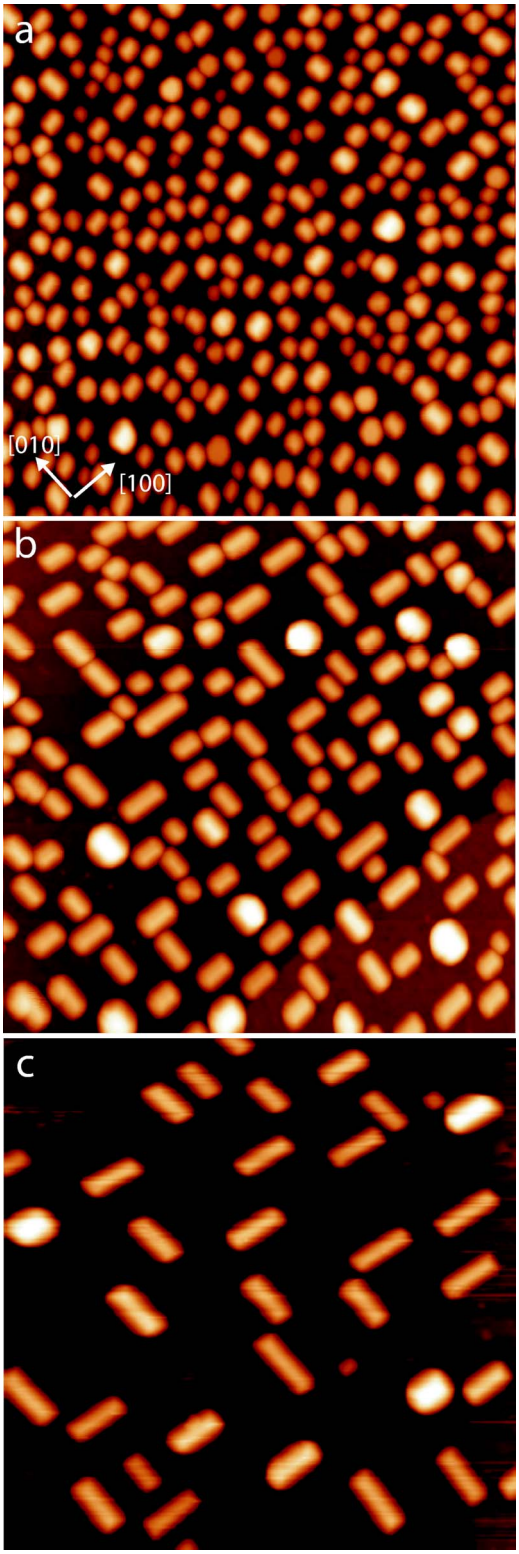

FIG. 1. (Color online) Pd deposition of around two monolayers onto $SrTiO_3(001)$-(2×1) substrates at different temperatures followed by 650 °C anneals gives rise to hut shaped nanocrystals as shown in the STM images (140×140 nm^2). (a) The sample was at room temperature during deposition ($V_s=+3.0$ V, $I_s=0.3$ nA). (b) The sample temperature during deposition was 320 °C ($V_s=+1.0$ V, $I_s=0.3$ nA). (c) The sample temperature during deposition was 415 °C.

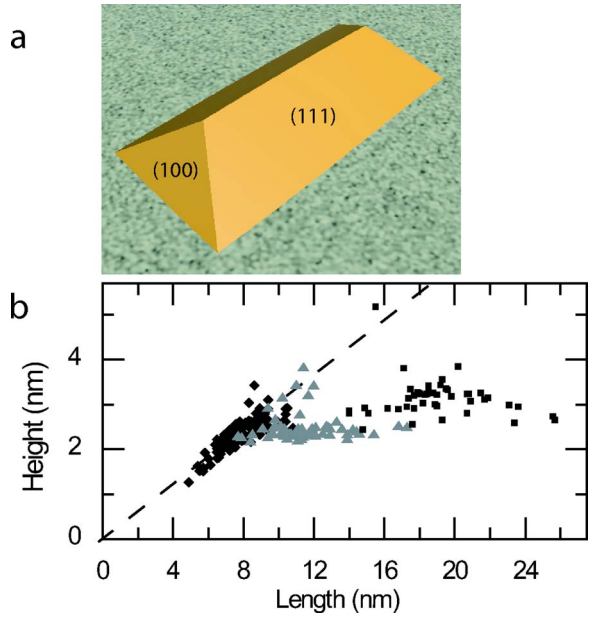

FIG. 2. (Color online) (a) Three-dimensional (3D) model of the hut shape. The large (111) facets have an angle of 35.3° relative to the substrate, and the angle with the small (100) facets is 45°. (b) Evolution of hut height with length for hut nanocrystals nucleated at room temperature (black diamonds), at 320 °C (gray triangles), and at 460 °C (black squares). All depositions were followed by a 45 min 650 °C anneal. The dashed line represent the equilibrium ratio.

Around 300 Pd clusters are present on the 140×140 nm^2 image in Fig. 1(a), but this number decreases to 130 in Fig. 1(b), and to 35 in Fig. 1(c). This demonstrates the decreasing number of nucleation sites as a function of increasing sample temperature during deposition.

Figure 2(b) shows the height evolution of the hut nanocrystals with their length for the different sample temperatures during Pd deposition, for huts nucleated at room temperature (black diamonds), at 320 °C (gray triangles), and 415 °C (black squares). The observed hut dimensions behave linearly for small islands nucleated at room temperature (black diamonds) and follow the equilibrium ratio (length of the base/height) $\ell/h\simeq3.48$ as previously reported.[1] The equilibrium ratio is indicated by the dashed line in the figure. At a 320 °C substrate deposition temperature, some of the huts are still at equilibrium (gray triangles) but the majority strongly deviate with a length which is longer than that at equilibrium. The huts grow preferentially along their length as opposed to their width or height, indicating that attachment to the (001) end facets is favored during growth. At a deposition temperature of 415 °C (black squares), the observed height reaches a constant value (~3.3 nm), meaning that at this temperature the huts are essentially only growing along their length.

B. Pd nanocrystals on $SrTiO_3(001)$-$c(4\times2)$: Hexagons and truncated pyramids

Around one monolayer of palladium was deposited on $SrTiO_3(001)$-$c(4\times2)$ surfaces at various temperatures and followed by subsequent 45 min anneals at 650 °C (Fig. 3).

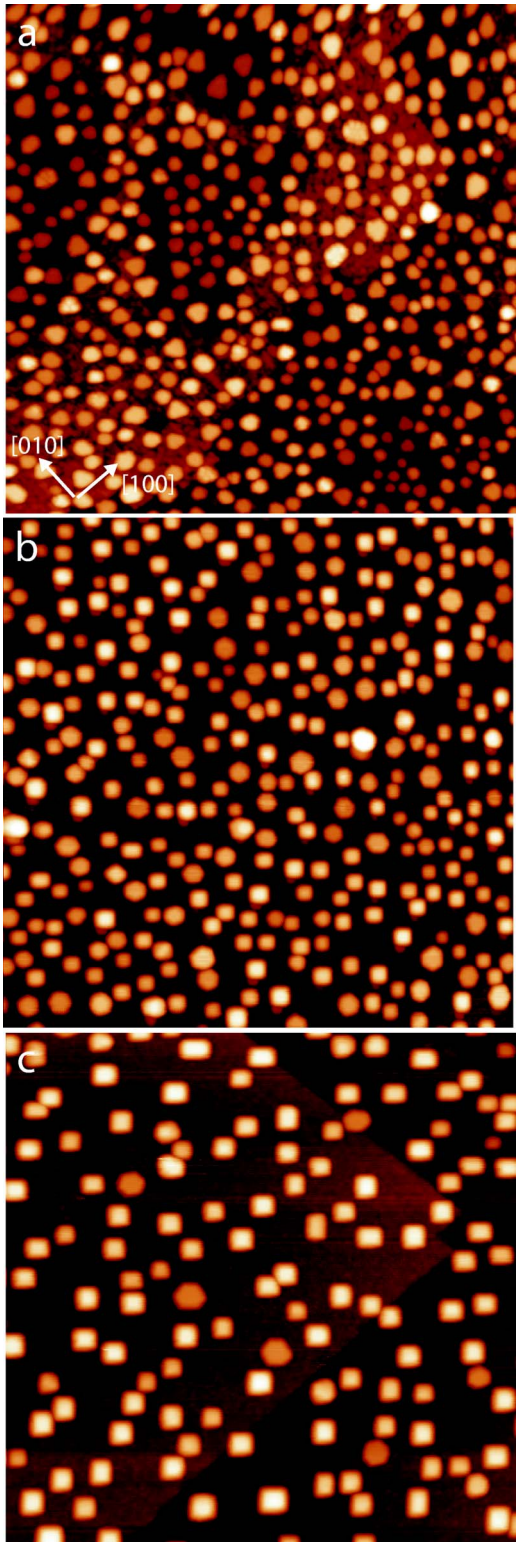

FIG. 3. (Color online) Pd deposition of around one monolayer onto $SrTiO_3(001)$-$c(4\times2)$ substrates at increasing temperatures followed by 650 °C anneals gives rise to two kinds of nanocrystal shapes. The hexagons and pyramids are shown in the STM images (140×140 nm^2, $V_s=+3.0$ V, $I_s=0.3$ nA). (a) The sample was at room temperature during deposition. (b) The sample temperature during deposition was 175 °C. (c) The sample temperature during deposition was 320 °C.

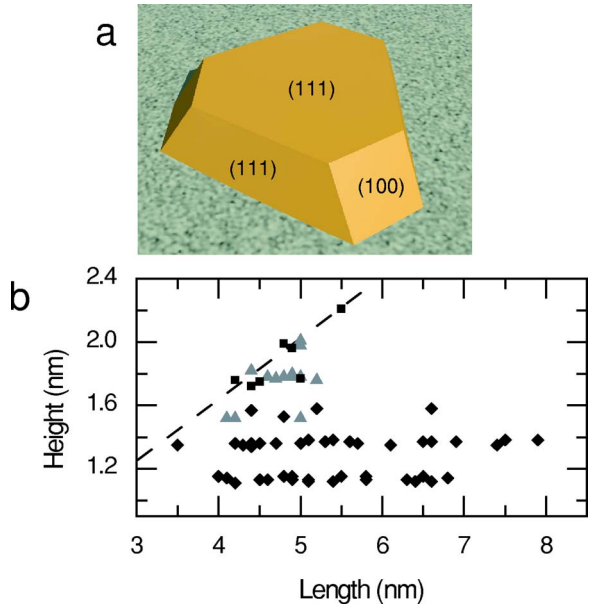

FIG. 4. (Color online) (a) 3D model of the hexagon shape. The (001) and (111) facets are indicated. (b) Evolution of hexagon height with length for hexagon nanocrystals nucleated at room temperature (black diamonds), at 320 °C (gray triangles), and at 460 °C (black squares). The depositions were followed by a 45 min 650 °C postanneal. The dashed line corresponds to the equilibrium ratio.

Figure 3(a) shows that Pd forms hexagonal nanocrystals when nucleated at room temperature. A model of this shape is presented in Fig. 4(a). The top of the hexagons is parallel to the substrate and its shape is typical of a truncated triangle which corresponds to a nanocrystal with a (111) top facet, three (111) side facets, and three (001) side facets. Hence the interface is $(111)_{Pd}\|(001)_{SrTiO_3}$,$[110]_{Pd}\|[110]_{SrTiO_3}$. At room temperature deposition, around 450 clusters are present on the 140×140 nm^2 image of which more than 99% have the shape of hexagonal discs.

If Pd is deposited on a $c(4\times2)$ substrate heated to 175 °C with the same 45 min postanneal at 650 °C as before, an additional nanocrystal shape appears as shown in Fig. 3(b). Around 320 Pd nanocrystals can be seen in the 140×140 nm^2 image, of which 85% have a square base and top facet (a truncated pyramid shape) as illustrated in Fig. 5(b). The other crystals have a hexagonal shape. The side facets of these truncated pyramid nanocrystals were measured at an angle of $\sim54°$ with respect to the substrate. This indicates that the pyramids have four (111) side facets, an (001) top facet, and an (001) interface, which allows cube on cube commensurate epitaxy with the $SrTiO_3(001)$ substrate and near perfect lattice matching. The interface crystallography is therefore $(001)_{Pd}\|(001)_{SrTiO_3}$,$[100]_{Pd}\|[100]_{SrTiO_3}$.

Figure 3(c) shows the surface after deposition of Pd on a $c(4\times2)$ substrate heated to 320 °C with the same 45 min postanneal at 650 °C. For this deposition temperature around 120 Pd nanocrystals can be seen in the 140×140 nm^2 image. The truncated pyramid shaped nanocrystal ratio increases to 95%.

For the same amount of Pd deposited on $SrTiO_3(001)$-$c(4\times2)$ (Fig. 3) an increase of substrate temperature during

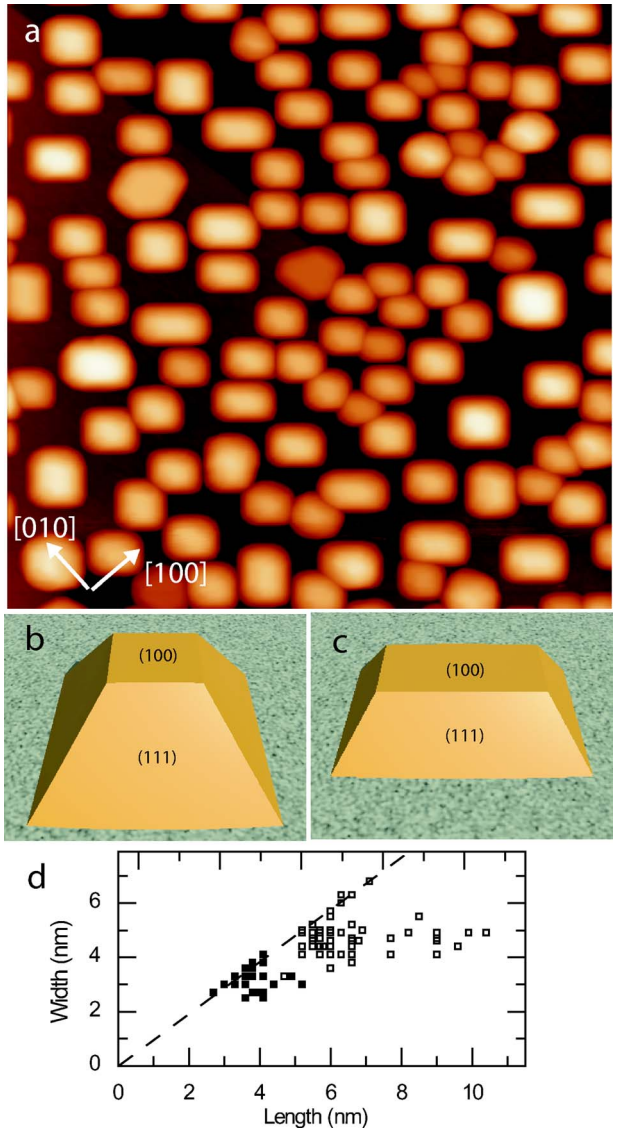

FIG. 5. (Color online) (a) Pd deposition of two monolayers onto a 320 °C $SrTiO_3(001)$-$c(4\times2)$ substrate followed by a 650 °C anneal gives rise to rectangular based clusters as shown in the STM image (140×140 nm^2, $V_s=+3.0$ V, $I_s=0.3$ nA). (b) 3D model of the square, and (c) elongated pyramid shapes with (001) and (111) facets indicated. (d) Evolution of pyramid width with length for pyramid nanocrystals nucleated at 320 °C followed by a 45 min 650 °C anneal for two different Pd concentrations. The black squares correspond to Fig. 3(c) (one monolayer) and the empty squares to Fig. 5(a) (two monolayers).

deposition yields a decrease of nucleation site density and an increase of nanocrystal size as expected. More surprisingly, a change in the nanocrystal shape is also seen.

Figure 4(b) shows the height evolution of the hexagonal nanocrystals with their length for the different sample temperatures during Pd deposition. Hexagons nucleated at room temperature are represented by black diamonds, at 320 °C as gray triangles, and at 415 °C as black squares. The cluster heights observed correspond to multiples of the Pd (111) lattice spacing. The quantization of cluster height is visible in Fig. 4(b). As shown in Fig. 3, the number of hexagons decreases with increasing deposition temperature, but Fig. 4(b) also shows that the height of the hexagons increases with temperature for a similar length. With increasing sample temperature during Pd deposition, the hexagon dimensions move to the hexagon equilibrium dimension determined as $\ell/h\simeq2.50$ and marked in Fig. 4(b) by a dashed line. This means that at low deposition temperatures hexagons grow preferentially along their length or width as opposed to their height, indicating that attachment to the side facets is favored during growth. At higher temperatures hexagons can grow along their height and move to the equilibrium shape, but their numbers are reduced.

Figure 5(a) shows the surface after deposition of around two monolayers of Pd on a $c(4\times2)$ substrate heated to 320 °C. The Pd is twice the amount previously deposited with the same flux. The same 45 min postanneal was carried out at 650 °C. For this temperature around 110 Pd nanocrystals can be seen in the 140×140 nm^2 image. The nanocrystal dimensions are bigger than observed in Fig. 3(c). A large majority of the nanocrystals in Fig. 3(c) have a square base, but in Fig. 5(a) only 57% have a square base. We find that 40% have a rectangular base, and 3% are hexagons. The rectangular based nanocrystals are elongated pyramids, which results in the shape shown schematically in Fig. 5(c).

Figure 5(d) shows a length to width plot of the pyramid nanocrystals formed at 320 °C for two different Pd concentrations [Figs. 3(c) and 5(a)]. The dimensions are taken along the top surface of the pyramid. As can be seen in Fig. 3(c), and represented by black squares in Fig. 5(d), the majority of the pyramid nanocrystals have a square base and top surface, which lie on the dashed line. Some nonequilibrium elongated pyramids with a rectangular base are also observed. As the volume of the nanocrystals is increased in Fig. 5(a), and represented by empty squares in Fig. 5(d), some pyramids are still square but the number of nanocrystals out of equilibrium has increased. The pyramids grow preferentially along one of their (111) side facets. The value of the width seems to reach a maximum at ~5.1 nm.

IV. DISCUSSION

Our experimental results show that Pd can form three distinct nanocrystal shapes on $SrTiO_3$ (001) depending on the surface reconstruction, the substrate temperature during deposition, and the Pd concentration. In our previous paper[1] we used a thermodynamic analysis of the nanocrystal energy as a function of shape and modified surface energy γ^*.[18] We showed that the huts and pyramids are stable, but that the hexagons are trapped in a metastable state. It was suggested that hexagon nanocrystal nucleation is highly dependent on kinetic as well as thermodynamic factors. In other words, hexagons are under certain circumstances the favored growth shape, and once nucleated as hexagons they cannot then overcome the energetic barrier required to assume the thermodynamically lowest energy truncated pyramid shape. In this paper we have further extended our study to include an analysis of the growth shapes of the hut and pyramid nanocrystals.

We have shown that on the (2×1) reconstructed surface of $SrTiO_3$ (001) Pd only forms hut shaped nanocrystals

within the temperature range we explored. We can vary the density of huts by adjusting the substrate temperature during deposition (Fig. 1). As long as nanocrystal nucleation is not defect mediated, the nucleation density is predicted to drop as the substrate temperature is increased, and this is indeed what we find. However, the effect of lower nanocrystal density is that the nanocrystals are on average larger. During the postanneal the nanocrystals undergo atomic reorganization to reach their equilibrium shape. At a constant temperature, the time it takes for a particle to reach its equilibrium shape is proportional to the fourth power of its radius.[20] It will therefore take substantially longer for larger particles to reach their equilibrium forms than for smaller particles. During the deposition stage of nanocrystal nucleation and growth the huts assume their growth shapes. We find that the postanneal is long enough for the small huts to reach their equilibrium shape, whereas for the large huts the anneal is not sufficiently long and they still display their growth shape. The growth shape for the huts is to have elongated (111) side facets, indicating that attachment during growth proceeds preferentially onto the (001) end facets. This is reasonable because the (001) end facets have a larger surface energy than the (111) side facets.[19]

The Pd nanocrystal nucleation and growth behavior on the $c(4\times2)$ reconstructed surface of $SrTiO_3$ (001) is very different from the (2×1) surface. Room temperature deposition results in hexagon nucleation, although the truncated pyramid shape has a lower energy (Fig. 3). The reason is thought to be because the (111) facet has the lowest surface energy, and submonolayer coverage would therefore favor a (111) layer. Once nucleated, the (111) monolayers grow preferentially by attachment to their sides resulting in hexagon shapes with a (111) interface that are flatter than their equilibrium form. The equilibrium form is reached for the small number of hexagons that are nucleated at higher deposition temperatures. The lowest energy shape for the $c(4\times2)$ surface is the truncated pyramid with an (001) interface. By adjusting the substrate deposition temperature it is possible to create nanocrystals of either shape, or a mixed shape distribution for intermediate temperatures (Fig. 3).

A natural question evolving from these observations is why we do not see hexagon nucleation for low temperature depositions on the (2×1) substrate. After all, the huts on the (2×1) surface have an (011) interface, which have a higher energy than the (001) surface. If (001) interface pyramids require elevated temperatures to nucleate, then should not this also be true for (011) interface huts? In fact, this may well be the case, but deposition temperatures below room temperature may be required to achieve hexagon nucleation on a (2×1) surface.

We now turn to the elongated growth shapes of the truncated pyramids. This shape evolves when one of the (111) growth facets is favored over the other three. As the attachment energies are the same for all the (111) side facets, elongation along one (111) facet must be due to anisotropy in the atomic flux impinging on the nanocrystal, as opposed to being a natural growth shape. The higher the density and area coverage of the nanocrystals, the greater the flux shielding effect one nanocrystal will have on its neighbors. This is why we see greater length to width anisotropy for higher Pd coverages (Fig. 5).

V. CONCLUSION

We have investigated the size and shape distributions of Pd nanocrystals on $SrTiO_3$ (001) supports. Our results show that depending on reconstruction and temperature during deposition three nanocrystal shapes can be created. We have studied the growth shapes of these nanocrystals: huts grow preferentially along their (001) end facets, hexagons grow preferentially in width rather than height, and truncated pyramids can become elongated if their density is sufficiently high. Due to its diversity in supported nanocrystal shape, Pd on $SrTiO_3$(001) should be regarded as a model system for the correlation of nanoparticle shape with optical and catalytic properties.

ACKNOWLEDGMENTS

The authors would like to thank the Royal Society and DSTL for funding and Chris Spencer (JEOL UK) for valuable technical support. We are also grateful to John A. Venables for illuminating discussions.

[1] F. Silly and M. R. Castell, Phys. Rev. Lett. **94**, 046103 (2005).
[2] V. Johanek, M. Laurin, A. W. Grant, B. Kasemo, C. R. Henry, and J. Libuda, Science **304**, 1639 (2004).
[3] M. Valden, X. Lai, and D. W. Goodman, Science **281**, 1647 (1998).
[4] P. L. Hansen, J. B. Wagner, S. Helveg, J. R. Rostrup-Nielsen, B. S. Clausen, and H. Topsoe, Science **295**, 2053 (2002).
[5] A. P. Alivisatos, Science **271**, 933 (1996).
[6] C. M. Lieber, Solid State Commun. **107** 607 (1998).
[7] G. Renaud, R. Lazzari, C. Revenant, A. Barbier, M. Noblet, O. Ulrich, F. Leroy, J. Jupille, Y. Borensztein, C. R. Henry, J.-P. Deville, F. Scheurer, J. Mane-Mane, and O. Fruchart, Science **300**, 1416 (2003).
[8] A. Kolmakov and D. W. Goodman, Chem. Rec. **2**, 446 (2002).
[9] J. Padilla and D. Vanderbilt, Surf. Sci. **418**, 64 (1998).
[10] T. Yoshimura, N. Fujimura, and T. Ito, J. Cryst. Growth **174**, 790 (1997).
[11] P. J. Moller, S. A. Komolov, and E. F. Lazneva, Surf. Sci. **425**, 15 (1999).
[12] F. Silly and M. R. Castell, J. Phys. Chem. B **109**, 12316 (2005).
[13] T. Conard, A.-C. Rousseau, L. M. Yu, J. Ghijsen, R. Sporken, R. Caudano, and R. L. Johnson, Surf. Sci. **359**, 82 (1996).
[14] D. A. Muller, N. Nakagawa, A. Ohtomo, J. L. Grazul, and H. Y. Hwang, Nature **430**, 657 (2004).
[15] T. Wagner, G. Richter, and M. Rühle, J. Appl. Phys. **89**, 2606 (2001).

[16] H. Nonomura, M. Nagata, H. Fujisawa, M. Shimizu, H. Niu, and K. Honda, Appl. Phys. Lett. **86**, 163106 (2005).
[17] M. R. Castell, Surf. Sci. **505**, 1 (2002).
[18] W. L. Winterbottom, Acta Metall. **15**, 303 (1967).
[19] M. Methfessel, D. Hennig, and M. Scheffler, Phys. Rev. B **46**, 4816 (1992).
[20] J. M. Bermond and J. A. Venables, J. Cryst. Growth **64**, 239 (1983).